Embedded nanograting-based waveplates for polarization control in integrated photonic circuits

Lammers, Kim ; Ehrhardt, Max; Malendevych, Teodor; Xu, Xiaoyu; Vetter, Christian; Alberucci, Alessandro; Szameit, Alexander; Nolte, Stefan

Published in:
Optical Materials Express

Link to article, DOI:
10.1364/OME.9.002560

Publication date:
2019

Document Version
Publisher's PDF, also known as Version of record

Research Article | Vol. 9, No. 6 / 1 June 2019 / Optical Materials Express 2560
Optical Materials EXPRESS

Embedded nanograting-based waveplates for polarization control in integrated photonic circuits

KIM LAMMERS,[1,*] MAX EHRHARDT,[2] TEODOR MALENDEVYCH,[1,3] XIAOYU XU,[1,4] CHRISTIAN VETTER,[1,5] ALESSANDRO ALBERUCCI,[1] ALEXANDER SZAMEIT,[2] AND STEFAN NOLTE[1,6]

[1]*Institute of Applied Physics, Abbe School of Photonics, Friedrich Schiller University Jena, Albert-Einstein-Str. 15, 07745 Jena, Germany*
[2]*Institut für Physik, Universität Rostock, Albert-Einstein-Str. 23, 18059 Rostock, Germany*
[3]*Laser and Plasma Laboratory, College of Optics and Photonics, University of Central Florida, 4304 Scorpius St, Orlando, FL 32186, USA*
[4]*DTU Fotonik, Technical University of Denmark, Ørsteds Pl., 2800 Kgs. Lyngby, Denmark*
[5]*FEMTO-ST Institute, Univ. Bourgogne Franche-Comté, CNRS, 15B Avenue des Montboucons, 25030 Besançon, Cedex, France*
[6]*Fraunhofer Institute for Applied Optics and Precision Engineering, Albert-Einstein-Str. 7, 07745 Jena, Germany*
[*]*kim.lammers@uni-jena.de*

Abstract: Femtosecond laser direct writing (FLDW) enables precise three-dimensional structuring of transparent host materials such as fused silica. With this technique, reliable integrated optical circuits can be written, which are also a possible candidate for future quantum technologies. We demonstrate the manufacturing of integrated waveplates with arbitrary orientations and various phase delays by combining embedded birefringent nanograting structures and FLDW waveguides in fused silica glass. These waveplates can be used both for classical applications and for quantum gates.

1. Introduction

Integrated optics is a key approach for realizing small and reliable optical circuits that can make use of various light properties. One of the fabrication methods for these integrated circuits is the so-called femtosecond laser direct writing method (FLDW) [1–3], known for its potential for rapid prototyping of three-dimensional small scale circuits [4]. To exploit the various degrees of freedom that light can offer, polarization control inside integrated optical circuits is crucial. There are various approaches for achieving this control in FLDW waveguides, including stress-induced birefringence [5–7], Bragg grating waveguides [8], birefringent directional couplers [9–14] and rotated waveguides [15]. Here, we propose a more compact while still integrated and reliable alternative to these polarization control approaches, based on the inscription of birefringent nanogratings.

There are typically three types of FLDW modifications that can be observed in silica glasses [16]: Firstly, at low energies isotropic refractive index changes used for creating waveguides are induced. Secondly, at high energies micro voids and defects are formed. Thirdly, at an intermediate energy range, structures with modulated oxygen concentration form [17]. If the fabrication laser polarization is linear and several hundred laser pulses per spot irradiate the material, strongly birefringent self-assembled nanogratings develop out of these structures [17–24]. The nanogratings are known to align perpendicular to the writing laser polarization with a period $p_{nano} \approx \lambda_w/(2n)$. Here, λ_w denotes the wavelength of the inscription laser and n refers to the refractive index of the modified material. When light of a suitable wavelength $\lambda \gg p_{nano}$

#364005 https://doi.org/10.1364/OME.9.002560
Journal © 2019 Received 1 Apr 2019; revised 24 Apr 2019; accepted 24 Apr 2019; published 14 May 2019

Optical Materials EXPRESS

passes through the nanograting, the latter acts as as an effective birefringent medium, because of the subwavelength periodic refractive index modulation. This property has been successfully used for creating bulk waveplates, attenuators and for optical data storage [21,25–29]. We investigated whether we can integrate waveplates made of nanogratings with femtosecond laser direct written waveguides as a compact approach for single photon polarization manipulation.

2. Manufacturing process

We used the FLDW method to write waveguides and nanogratings into polished fused silica samples. The writing laser system was a fiber laser (Satsuma, Amplitude Systemes), emitting pulses at 1030 nm, then undergoing a frequency doubling to a wavelength of 515 nm. A cylindrical telescope with lenses of −50 mm and 150 mm focal lengths was used for astigmatic beam shaping, which is a well-known technique for creating cylindrically symmetric waveguides [30–32]. The astigmatic beam was also used for writing nanogratings. The 300 fs long laser pulses were focused using a 20x-objective (NA = 0.4) whilst the sample was translated through the beam focus using a nanopositioning system (Aerotech ANT130-XY), as shown in Fig. 1.

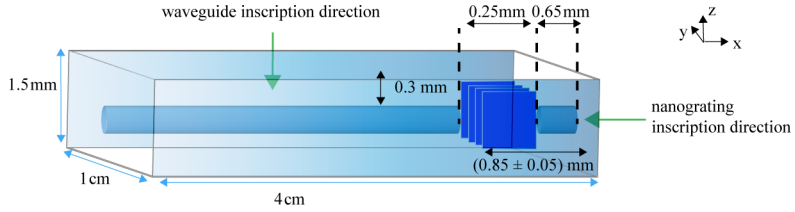

Fig. 1. Sketch of the sample. The nanograting depiction is not to scale; typical nanograting layers had a thickness of 50 µm to 110 µm, depending on the fabrication parameters. The nanogratings started 0.8 mm to 0.9 mm from the sample's rear end. The waveguides were inscribed 0.3 mm below the surface.

The sample sizes were 0.15 cm × 1 cm × 4 cm (Fig. 1). The nanogratings were inscribed using fs-pulses propagating along x into the y-z-plane 0.8 mm to 0.9 mm below the end facet. Afterwards, the waveguides were inscribed in the x-y-plane 0.3 mm below the surface. In consequence the waveguide and the nanograting planes crossed perpendicularly, as can be seen in Fig. 1. All together, the structure consists of a 3.1 cm long waveguide section, a 0.25 mm long gap, into which the nanograting is inscribed, followed by another 0.65 mm long waveguide section. The nanograting on the transverse y-z-plane is much wider than the waveguide, so it can be assumed infinitely extended. Between the waveguide sections and the nanogratings is unmodified fused silica. This unmodified region acts as a buffer to avoid waveguides being inscribed into previously written nanogratings. This method of leaving gaps in waveguides has been successfully applied before for manipulating the phase accumulated inside the waveguide [33].

The intrinsic form birefringence of the nanogratings changes the polarization state of light transmitted through this combination. By doing so, the nanograting acts as a waveplate. The strength of the nanograting birefringence was set by changing the pulse energy. The orientation of the optical axis was set by rotating the laser polarization for nanograting inscription.

The writing parameters of the waveguides were set to 600 mm/min writing speed, 100 kHz repetition rate and 0.12 µJ pulse energy. The waveguides themselves exhibited a birefringent phase delay $\Delta\phi$ between the horizontal and vertical polarization of around $0.037\,\pi\,\mathrm{cm}^{-1}$ for light of wavelength $\lambda = 808$ nm, corresponding to an intrinsic birefringence of $\Delta n = \Delta\phi\lambda/(2\pi) = 1.5 \times 10^{-6}$. The overall losses of the waveguides were measured to be 12.9±0.4 dB, of which 0.3 dB can be attributed to the Fresnel losses, 4.9 dB to coupling losses at the waveguide entry and 1.9 dB losses from the objective after the sample, leaving 1.5±0.1 dB/cm for the propagation

Optical Materials EXPRESS

losses. However, the focus of our work was not to minimize losses. Previous publications have shown that average propagation losses of 0.1 dB/cm at 777 nm wavelength can be achieved in fused silica FLDW waveguides [34]. Furthermore, other publications have demonstrated approaches of minimizing insertion losses [35].

In addition, the waveguides exhibited polarization dependent losses. The transmission of horizontally polarized light through a 4 cm long waveguide is 6 % lower than the transmission of vertically polarized light; in other words the normalized linear dichroism is 6 %. An exemplary profile of mode fields is given in Fig. 2 and the corresponding refractive index profile in Fig. 3.

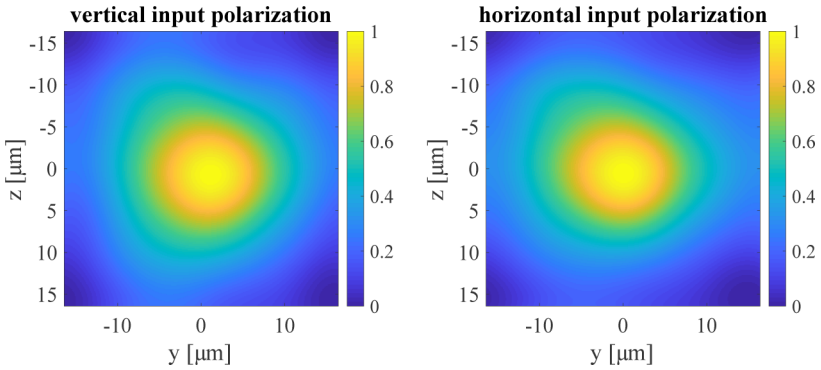

Fig. 2. Normalized near field images of mode fields when vertically or horizontally polarized light at $\lambda = 808$ nm is launched into the waveguide. The image was filtered using a Butterworth filter. The setup for measuring this mode field corresponds to the setup in Fig. 4, whereby the power meter is replaced by a CCD camera.

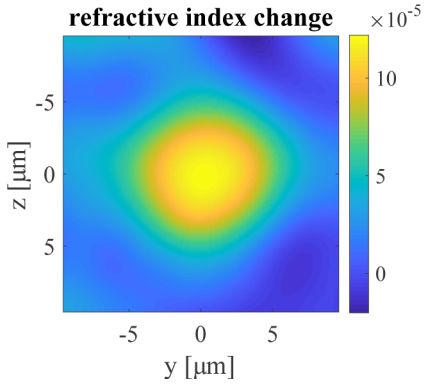

Fig. 3. Refractive index profile calculated from mode field images shown in Fig. 2, based on the technique presented in [36].

It is known in linear optical quantum computing that waveplates as phase shifters can be used to create single qubit quantum gates [37–39]. For suitable writing parameters, the birefringence of the nanograting-waveguide combination matches the required birefringence for linear optical quantum gates, as will be demonstrated below.

3. Characterization method

The birefringence induced phase delay of light transmitted through the FLDW structures was measured using two different methods: For the nanogratings alone, a commercial polarimeter

Optical Materials EXPRESS

(ilis StrainMatic) was used. For the nanograting-waveguide-combinations, a crossed polarizer setup was used (Fig. 4), similar to the one described in [20]. In the crossed polarizer setup, the sample is positioned between a rotatable $\lambda/2$ plate and a rotatable analyzer. A subsequent power meter measures the power transmitted through the polarizer. The $\lambda/2$ plate sets the input polarization. The analyzer orientation is kept at 90° to the input polarization (crossed orientation). Both the analyzer and the $\lambda/2$ plate are rotated. If there is no anisotropic sample in the setup, no power is transmitted through to the power meter. If an anisotropic sample is placed between the analyzer and the $\lambda/2$-plate however, the birefringence of that sample changes the polarization state of light transmitted through the sample. This can be measured as a change of output power through the crossed polarizer configuration. If the sample is a linear retarder, the formula for the transmitted power normalized to the overall output power T_{norm} depends on the input polarization orientation ϕ as follows:

$$T_{norm} = A \sin^2[2(\phi - \phi_0)]. \tag{1}$$

Here, the amplitude A is a measure of the existing birefringence. The angle ϕ_0 accounts for the orientation of the optical axis of the sample studied [40]. By measuring the transmitted output power versus the input polarization and fitting the acquired data to a sine curve, we can retrieve the birefringence of our structures, modeling them as linear retarders without any polarization dependent loss. The birefringence induced phase delay δ relates to the measured amplitude A of Eq. (1) via

$$|\delta| = |\arccos(1 - 2A)|. \tag{2}$$

The measurements were performed using laser light of 808 nm wavelength, to suit the wavelength of the single photon measurements described below. We are aware that nanogratings do exhibit asymmetric losses, which are not covered by this model [19,41,42]. A simple simulation based on asymmetric loss measurements yielded a deviation of the derived birefringence due to this effect of 0.05π.

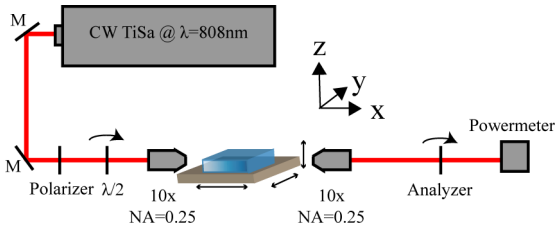

Fig. 4. Sketch of the characterization setup.

4. Results

4.1. Influence of writing parameters on the structure properties

It has been experimentally verified that, with rising pulse energy over a range of 0.4 µJ to 0.9 µJ, the phase delay induced by the nanogratings increases together with their thickness (Fig. 5). The structures were fabricated by single height scans, so the thicknesses and the phase delays are linked. The writing velocity was kept constant at 15 mm/min and the line separation was set to 1 µm. The pulse energy dependence can be used to find a suitable nanograting strength for fabricating quantum gates.

As a first step to creating quantum gates, the dependence of the nanograting-waveguide-combination on the pulse energy used for inscription of the nanogratings was investigated. The writing parameters of the waveguides were kept fixed. It was found that the overall phase delay in the nanograting-waveguide-combination was mainly determined by the nanograting phase delay

Optical Materials EXPRESS

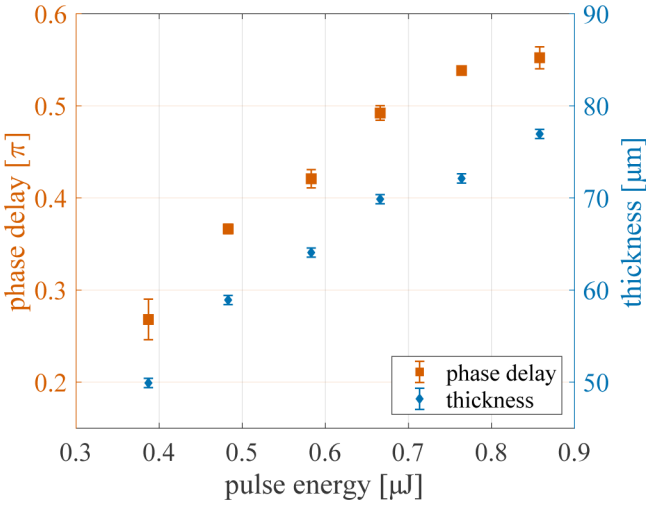

Fig. 5. Measured phase delay induced by nanogratings for light of 808 nm wavelength and thickness of nanograting layers for various writing laser pulse energies. The gratings were written at 100 kHz repetition rate and 15 mm/min scanning speed. Error bars of the phase delay induced by the nanogratings refer to the standard deviation of the birefringence measured over a nanograting area of 0.26 mm × 0.26 mm. Error bars of the layer thickness refer to the measurement tolerances.

(Fig. 6). Nevertheless, a slight offset of about 0.01π to 0.05π was visible. This might be due to the remaining intrinsic birefringence of the 4 cm long waveguide (as described in section 2), as well as due to additional stress birefringence caused around these waveguides by the additional nanograting. Losses induced by single layers of nanogratings are on the order of 1.2 dB to 1.4 dB.

In a next step, the polarization of the writing laser was rotated by a few degrees for a set of nanogratings fabricated with otherwise constant writing parameters. Waveguides were added to the nanogratings and the overall birefringence was measured. It is observed that the optical axis of the system rotated with the polarization of the writing laser (Fig. 7). The rotation of the optical axis is a crucial element in having full freedom for creating the required phase retardations for quantum gates. At the same time, the strength of the phase retardation changed, showing a preferred development of nanogratings for certain polarizations (Fig. 7). The variation in birefringence strength for different polarizations was also visible for the nanogratings alone. The change of the total birefringence is stronger than the change of only the nanogratings. The reasons for this will have to be clarified in future work. Possible explanations could be symmetry breaking due to the scanning direction while writing, an orientation dependent coupling of waveguide and nanograting, or parasitic stress induced birefringence effects around the nanograting structure (the orientation of the nanogratings have significant effect on the stress distribution in the material [43,44]). The orientation dependence of the induced birefringence has to be accounted for when selecting suitable writing parameters.

Summarizing, we have shown the control over two degrees of freedom: The orientation of the optical axis and the amount of phase delay induced by the structures. This has applications both in the classical regime as arbitrary waveplates, and in the quantum regime, since any phase and polarization transformation can be represented by Jones matrices [45], and some Jones matrices correspond to single qubit quantum gates [38].

FLDW chips are a popular platform for quantum operations [7,15,46]. The functionalization of our structures is only a few hundred micrometers wide, surpassing some former approaches for fabricating waveplates in compactness (compare e.g. [7,15], where the required defect line

Optical Materials EXPRESS

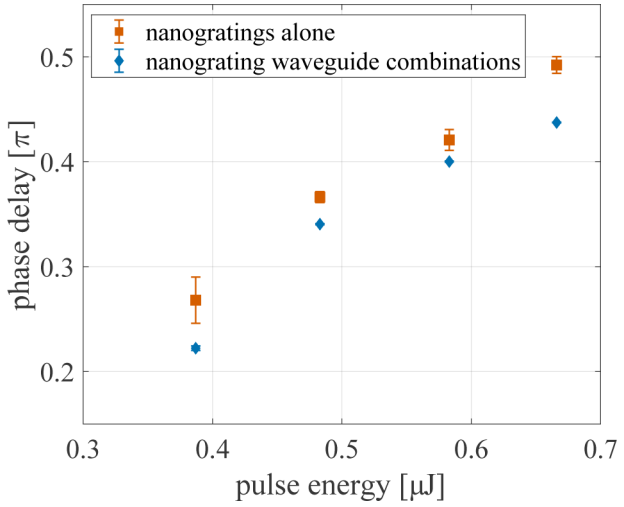

Fig. 6. Measured phase delay of the combination of nanogratings with waveguides compared to the measured phase delay for the nanogratings, for various writing laser pulse energies, at a wavelength of 808 nm. Only the writing laser pulse energy for the nanograting was altered, while the writing parameters of the waveguides were kept the same for all measurement points. The gratings were written at 100 kHz repetition rate and 15 mm/min scanning speed. Error bars refer to the standard deviation of the birefringence measured over a nanograting area of 0.26 mm × 0.26 mm. Error bars of the combination measurements refer to the fit accuracies.

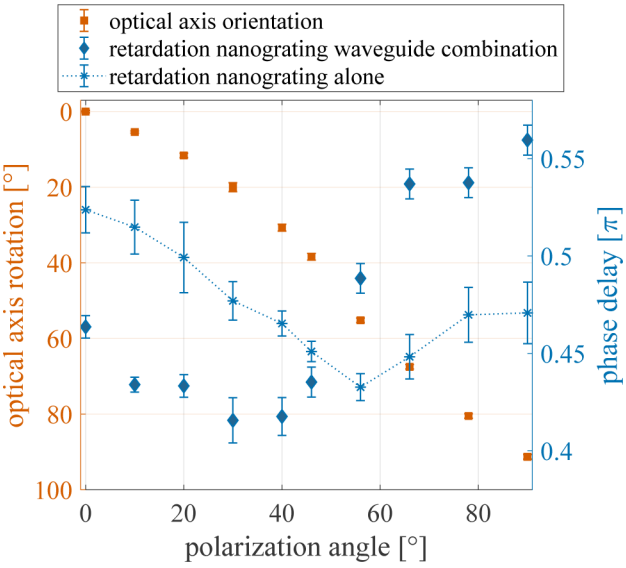

Fig. 7. Influence of writing laser polarization angle on the optical axis and induced phase delay of nanograting-waveguide-combinations. Error bars are based on the standard deviation of the polarimeter measurement and on fit accuracies. The dotted line is a guide for the eye to distinguish the data sets. An orientation of 0° corresponds to horizontally polarized light. The nanogratings were written at 100 kHz, 15 mm/min scannning speed and 0.8 μJ pulse energy.

Optical Materials EXPRESS

or waveguide segments were in the range of centimeters), while allowing a full rotation of the optical axis. As an application example, we will demonstrate the fabrication of specific quantum gates. Several gates are of special interest, among them the quantum gates Pauli-x (σ_x), Pauli-y (σ_y) and Pauli-z (σ_z) with a transmission matrix corresponding to the Pauli matrices:

$$\sigma_x = \begin{bmatrix} 0 & 1 \\ 1 & 0 \end{bmatrix}; \qquad \sigma_y = \begin{bmatrix} 0 & -i \\ i & 0 \end{bmatrix}; \qquad \sigma_z = \begin{bmatrix} 1 & 0 \\ 0 & -1 \end{bmatrix}. \tag{3}$$

They are interesting, because in absence of losses any 2x2 matrix can be written as a superposition of Pauli matrices and the identity matrix. However, the Pauli-y gate can also be created by a combination of Pauli-x, Pauli-z gates and a very specific overall phase shift [38], therefore we will limit our investigations to Pauli-x and Pauli-z gates.

At the same time, the so-called Pi/8th gate Π_{8th} and Hadamard gate H are of special interest, because they form a universal set for one-qubit quantum computation [47]. Note that the name of the Pi/8th gate is historical and does not refer to the required phase delay. Their matrices are as follows [38]:

$$H = \frac{1}{\sqrt{2}} \begin{bmatrix} 1 & 1 \\ 1 & -1 \end{bmatrix}; \qquad \Pi_{8th} = \begin{bmatrix} 1 & 0 \\ 0 & e^{i\pi/4} \end{bmatrix}. \tag{4}$$

4.2. Classical characterization of quantum gates

For the two cases when the optical axis of the nanograting and the waveguide are oriented parallel or perpendicular to each other, we were able to reach birefringence induced phase delays close to π and $\pi/4$, corresponding to the phase delay requirements for Pauli-z and Pi/8th quantum gates, respectively [38] (Fig. 8). Additionally, we were able to fabricate a Pauli-x gate, whose optical axis was rotated by 45° and whose induced phase delay was close to π. Finally, a Hadamard gate was created (Fig. 8). Hereby, we have demonstrated the possibility of creating quantum gates, which can be realized with different phase delays as well as different orientations. The nanogratings for the Pi/8th and the Pauli-z gate were inscribed using horizontally polarized light, at a writing velocity of 15 mm/min and a repetition rate of 100 kHz. In case of the Pi/8th gate, a single layer of nanogratings created with a pulse energy of 0.4 µJ was used. The thickness of this nanograting layer was 0.05 mm. For the Pauli-z gate, two nanograting layers with a thickness of 0.07 mm and a gap along the waveguide direction of 0.03 mm were used. The writing pulse energy was 0.8 µJ. For the Pauli-x gate, the same writing velocity and repetition rate was used, but the writing polarization was diagonally polarized and the pulse energy was 0.7 µJ. Like before, two layers of nanogratings with a thickness of 0.06 mm and a gap of 0.04 mm were used. The second layer was required to reach sufficient phase delays. The nanograting for the Hadamard gate was created using pulses of 0.8 µJ and a polarization rotated to 112.5°, to reach a suitable orientation of the optical axis. Again, this was a two layer gate, with each nanograting layer having a thickness of 0.06 mm and a gap of 0.04 mm in between.

In these plots the measurement points as well as the corresponding sine square fit to the measurement points are displayed. For the Pi/8th gate the fit yielded an amplitude of $A = 0.133$, corresponding to a birefringent phase delay of 0.24π, the Pauli-z gate fit yielded an amplitude of $A = 0.992$, corresponding to a birefringence of 0.94π and the Pauli-x gate fit yielded an amplitude of $A = 0.987$, corresponding to a birefringence of 0.93π, whilst the Hadamard gate gave an amplitude of $A = 0.978$, equaling a birefringence of 0.91π. The losses of these gates were determined in the setup of Fig. 8, but replacing the single photon source with a crystal. Overall losses were on the order of 13.2 dB to 14.8 dB, of which around 7.1 dB are due to in- and out-coupling and Fresnel reflection losses, 5.4 dB to 6.2 dB are losses in the waveguide structures, leaving up to 2.3 dB losses caused from the nanograting structures. However, we would like to

Optical Materials EXPRESS

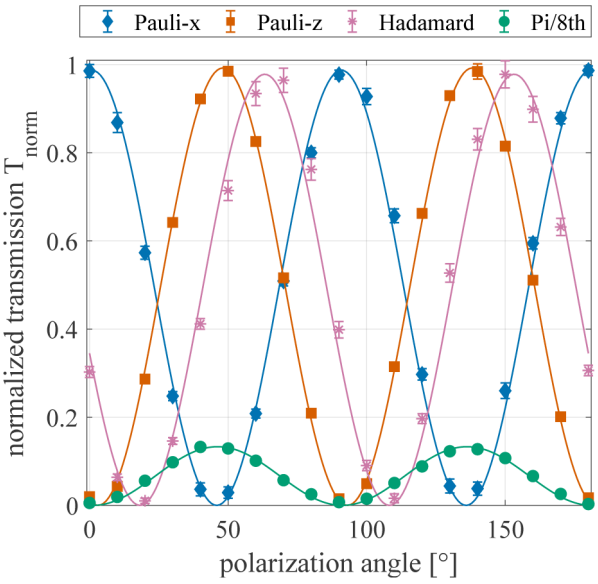

Fig. 8. Normalized transmission through crossed polarizers of Eq. (1) for the Pauli-x, Pauli-z, Pi/8th and Hadamard gates with according sine square fit function. Error bars are based on the standard deviation of at least 18 measurements at each point.

stress that no efforts were made to reduce the losses. Other publications have shown that losses induced by nanogratings can be limited to below 0.5 dB [48].

4.3. *Single photon characterization of quantum gates*

In a next step the quantum matrices of these gates were determined using single photon measurements. The corresponding setup is depicted in Fig. 9. To produce these single photon pairs, spontaneous parametric down conversion of a BiBo crystal was used. The photons were coupled into single mode fibers. The first photon was butt-coupled into the sample, whilst the second photon served as a triggering signal for the first. Hereby, it was ensured that single photons were used and dark counts were omitted. To make sure that indistinguishable photons were measured, the Hong-Ou-Mandel Dip was measured in advance [49]. The polarization state of the first photon was set using fiber polarization controllers. Degrees of polarization of >99% were achieved. The polarization state after the sample was measured in the horizontal/vertical $|H\rangle/|V\rangle$ basis using a polarizing beam splitter, as well as in the left circular/right circular $|L\rangle/|R\rangle$ basis by adding a $\lambda/4$ oriented at ±45° in front of the beam splitter. The absolute values of the matrix entries were directly determined from the $|H\rangle/|V\rangle$-measurements after horizontally or vertically polarized photons were sent into the sample. To determine the phases, all four options of input states ($|H\rangle/|V\rangle/|L\rangle/|R\rangle$), were measured both in the $|H\rangle/|V\rangle$ and in the $|L\rangle/|R\rangle$ basis. These values were used in a residual sum of squares minimization, to retrieve the remaining phases. The phase of the first matrix entry was set to zero in all cases, omitting any overall phases.

The retrieved matrices are listed in Table 1 and displayed in Fig. 10. The error bars result from the statistics of multiple measurements and from poissonian statistics of each measurement.

The corresponding fidelities ($F^{|\psi\rangle} = |\langle\psi|M^*_{ideal}M_{exp}|\psi\rangle|^2$ [50], with M^*_{ideal} being the conjugate transpose of the theoretical matrix and M_{exp} being the experimentally retrieved matrix) were calculated for the measurement matrices with the smallest residual sum of squares. They are listed in Table 2.

Optical Materials EXPRESS

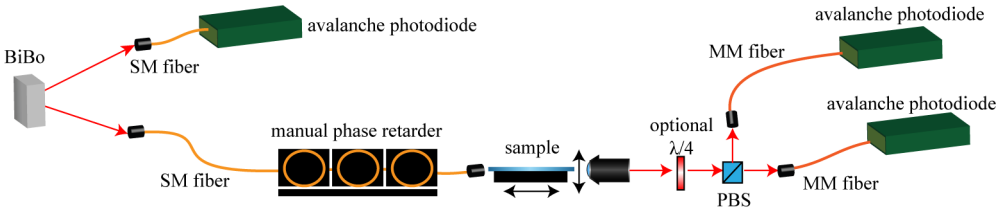

Fig. 9. Single photon measurement setup. The wavelength of the single photon source is $\lambda = 815$ nm, close to the characterization wavelength of Fig. 4. (PBS = Polarizing Beam Splitter, MM = Multi-Mode, SM = Single Mode)

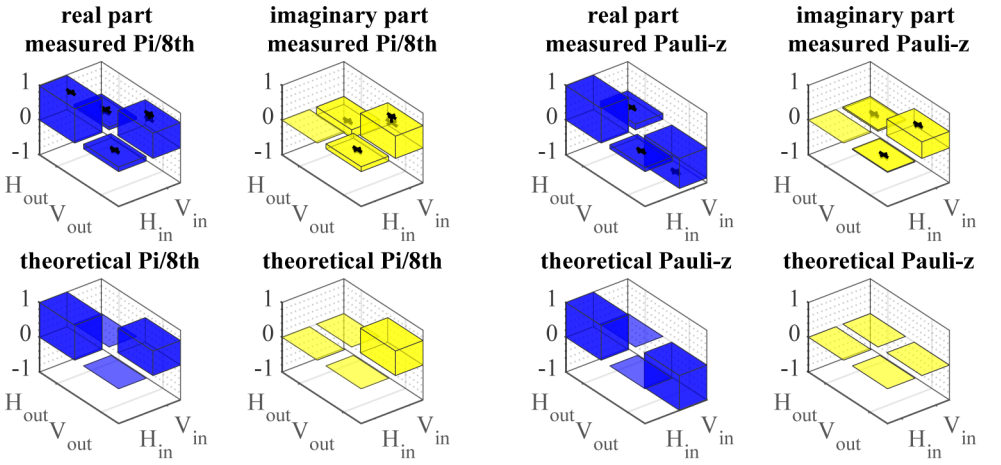

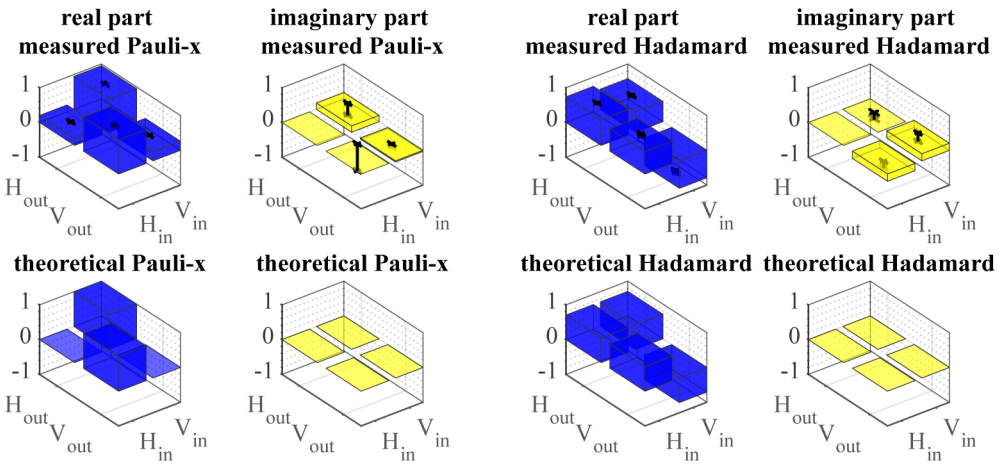

Fig. 10. Retrieved matrices for the Pi/8th, Pauli-z, Pauli-x and Hadamard gates.

Optical Materials EXPRESS

Table 1. Reconstructed matrices of quantum gates.

Gate	Matrix
Pi/8th	$\begin{matrix}(0.981 \pm 0.001) & (0.243 \pm 0.005) \cdot e^{-i\cdot(0.4\pm0.05)\pi} \\ (0.194 \pm 0.006) \cdot e^{i\cdot(0.2\pm0.1)\pi} & (0.970 \pm 0.001) \cdot e^{i\cdot(0.23\pm0.04)\pi}\end{matrix}$
Pauli-z	$\begin{matrix}0.993 & (0.168 \pm 0.003) \cdot e^{-i\cdot(0.09\pm0.03)\pi} \\ (0.119 \pm 0.003) \cdot e^{-i\cdot(0.05\pm0.08)} & (0.986 \pm 0.001) \cdot e^{i\cdot(0.85\pm0.03)\pi}\end{matrix}$
Pauli-x	$\begin{matrix}(0.201 \pm 0.005) & (0.965 \pm 0.002) \cdot e^{i\cdot(0.06\pm0.06)\pi} \\ (0.980 \pm 0.001) \cdot e^{i\cdot(0.01\pm0.12)\pi} & (0.262 \pm 0.007) \cdot e^{-i\cdot(0.04\pm0.05)\pi}\end{matrix}$
Hadamard	$\begin{matrix}(0.738 \pm 0.002) & (0.579 \pm 0.003) \cdot e^{-i\cdot(0.01\pm0.04)\pi} \\ (0.674 \pm 0.003) \cdot e^{-i\cdot(0.09\pm0.06)\pi} & (0.816 \pm 0.002) \cdot e^{-i\cdot(0.92\pm0.05)\pi}\end{matrix}$

Table 2. Calculated fidelities.

Gate	Fidelity $F^{\lvert H\rangle,\lvert V\rangle}$
Pi/8th	0.952 ± 0.011
Pauli-z	0.979 ± 0.007
Pauli-x	0.930 ± 0.031
Hadamard	0.966 ± 0.008

As can be seen, some deviation from the ideal matrices are still present. The cause of this is not quite clear, possibly some inhomogeneities in the nanograting structures could be the reason. Further reducing the writing speed during fabrication and therefore homogenizing the nanograting structure might be suitable to improve this. For the matrices corresponding to waveplates with tilted axes two additional error sources come into play. Firstly, there is the remaining waveguide birefringence (as described in section 2) that changes the light's polarization state in an unfavorable manner. Secondly, there is also the unpreferred development of nanogratings which are neither in writing direction nor at 90° orientation to it. Therefore, finding ways to further lower the waveguide birefringence (e.g. by annealing) and writing the nanogratings in the direction of the optical axis might further improve the performance of future gates fabricated with the here proposed method.

5. Conclusion

We investigated the possibility of polarization control inside FLDW waveguides by adding embedded nanograting planes across the waveguide. We demonstrated dependencies of the nanograting birefringence on the inscription parameters, and the feasibility of creating quantum gates using this approach. Therefore we demonstrated the usability of this approach for creating integrated waveplates of arbitrary phase delays and arbitrary orientations. Four quantum gates were investigated: The Pi/8th gate, the Pauli-x gate, Pauli-z gate and the Hadamard gate. The corresponding quantum gate matrices were retrieved using single photon measurements, yielding fidelities of $F^{|H\rangle,|V\rangle} = (0.930 \pm 0.031)$ and higher. However, some matrix values still deviated noticeably from the theoretically desired values. Further optimization of the fabrication parameters could help relieve this problem. Apart from further improving the performance of these structures, it would be of great interest to combine them with other integrated structures, showing their applicability in more complex integrated optical circuits.

Optical Materials EXPRESS

Funding

Deutsche Forschungsgemeinschaft (DFG) (grant SZ 276/12-1, International Research Training Group GRK 2101); Bundesministerium für Bildung und Forschung (BMBF) (Max Planck School of Photonics); Horizon 2020 Framework Programme (H2020) (grant agreement No 800942); Alfried Krupp von Bohlen und Halbach-Stiftung.

Acknowledgments

K.L. is part of the Max Planck School of Photonics supported by BMBF, Max Planck Society, and Fraunhofer Society. This project has received funding from the European Union's Horizon 2020 research and innovation programme under grant agreement No 800942. AS gratefully acknowledges financial support from the Alfried Krupp von Bohlen und Halbach Foundation.

Disclosures

The authors declare that there are no conflicts of interest related to this article.

References

1. K. M. Davis, K. Miura, N. Sugimoto, and K. Hirao, "Writing waveguides in glass with a femtosecond laser," Opt. Lett. **21**(21), 1729 (1996).
2. K. Miura, J. Qiu, H. Inouye, T. Mitsuyu, and K. Hirao, "Photowritten optical waveguides in various glasses with ultrashort pulse laser," Appl. Phys. Lett. **71**(23), 3329–3331 (1997).
3. J. W. Chan, T. Huser, S. Risbud, and D. Krol, "Modification of the fused silica glass network associated with waveguide fabrication using femtosecond laser pulses," Appl. Phys. A **76**(3), 367–372 (2003).
4. T. Meany, M. Gräfe, R. Heilmann, A. Perez-Leija, S. Gross, M. J. Steel, M. J. Withford, and A. Szameit, "Laser written circuits for quantum photonics," Laser Photonics Rev. **9**(4), 363–384 (2015).
5. L. A. Fernandes, J. R. Grenier, P. R. Herman, J. S. Aitchison, and P. V. Marques, "Stress induced birefringence tuning in femtosecond laser fabricated waveguides in fused silica," Opt. Express **20**(22), 24103–24114 (2012).
6. L. A. Fernandes, J. R. Grenier, P. V. Marques, J. S. Aitchison, and P. R. Herman, "Strong birefringence tuning of optical waveguides with femtosecond laser irradiation of bulk fused silica and single mode fibers," J. Lightwave Technol. **31**(22), 3563–3569 (2013).
7. R. Heilmann, M. Gräfe, S. Nolte, and A. Szameit, "Arbitrary photonic wave plate operations on chip: realizing hadamard, pauli-x, and rotation gates for polarisation qubits," Sci. Rep. **4**(1), 4118 (2014).
8. L. A. Fernandes, J. R. Grenier, P. R. Herman, J. S. Aitchison, and P. V. Marques, "Femtosecond laser writing of waveguide retarders in fused silica for polarization control in optical circuits," Opt. Express **19**(19), 18294–18301 (2011).
9. L. A. Fernandes, J. R. Grenier, P. R. Herman, J. S. Aitchison, and P. V. Marques, "Femtosecond laser fabrication of birefringent directional couplers as polarization beam splitters in fused silica," Opt. Express **19**(13), 11992–11999 (2011).
10. A. Crespi, R. Ramponi, R. Osellame, L. Sansoni, I. Bongioanni, F. Sciarrino, G. Vallone, and P. Mataloni, "Integrated photonic quantum gates for polarization qubits," Nat. Commun. **2**(1), 566 (2011).
11. I. Pitsios, F. Samara, G. Corrielli, A. Crespi, and R. Osellame, "Geometrically-controlled polarisation processing in femtosecond-laser-written photonic circuits," Sci. Rep. **7**(1), 11342 (2017).
12. I. Dyakonov, M. Y. Saygin, I. Kondratyev, A. Kalinkin, S. Straupe, and S. Kulik, "Laser-written polarizing directional coupler with reduced interaction length," Opt. Lett. **42**(20), 4231–4234 (2017).
13. J. Zeuner, A. N. Sharma, M. Tillmann, R. Heilmann, M. Gräfe, A. Moqanaki, A. Szameit, and P. Walther, "Integrated-optics heralded controlled-not gate for polarization-encoded qubits," NPJ Quantum Inf. **4**(1), 13 (2018).
14. C.-Y. Wang, J. Gao, and X.-M. Jin, "On-chip rotated polarization directional coupler fabricated by femtosecond laser direct writing," Opt. Lett. **44**(1), 102–105 (2019).
15. G. Corrielli, A. Crespi, R. Geremia, R. Ramponi, L. Sansoni, A. Santinelli, P. Mataloni, F. Sciarrino, and R. Osellame, "Rotated waveplates in integrated waveguide optics," Nat. Commun. **5**(1), 4249 (2014).
16. K. Itoh, W. Watanabe, S. Nolte, and C. B. Schaffer, "Ultrafast processes for bulk modification of transparent materials," MRS Bull. **31**(08), 620–625 (2006).
17. Y. Shimotsuma, P. G. Kazansky, J. Qiu, and K. Hirao, "Self-organized nanogratings in glass irradiated by ultrashort light pulses," Phys. Rev. Lett. **91**(24), 247405 (2003).
18. L. Sudrie, M. Franco, B. Prade, and A. Mysyrowicz, "Writing of permanent birefringent microlayers in bulk fused silica with femtosecond laser pulses," Opt. Commun. **171**(4-6), 279–284 (1999).
19. P. Kazansky, H. Inouye, T. Mitsuyu, K. Miura, J. Qiu, K. Hirao, and F. Starrost, "Anomalous anisotropic light scattering in ge-doped silica glass," Phys. Rev. Lett. **82**(10), 2199–2202 (1999).

Optical Materials EXPRESS

20. P. Yang, G. R. Burns, J. Guo, T. S. Luk, and G. A. Vawter, "Femtosecond laser-pulse-induced birefringence in optically isotropic glass," J. Appl. Phys. **95**(10), 5280–5283 (2004).
21. L. P. R. Ramirez, M. Heinrich, S. Richter, F. Dreisow, R. Keil, A. V. Korovin, U. Peschel, S. Nolte, and A. Tünnermann, "Tuning the structural properties of femtosecond-laser-induced nanogratings," Appl. Phys. A **100**(1), 1–6 (2010).
22. S. Richter, M. Heinrich, S. Döring, A. Tünnermann, and S. Nolte, "Formation of femtosecond laser-induced nanogratings at high repetition rates," Appl. Phys. A **104**(2), 503–507 (2011).
23. Y. Shimotsuma, K. Miura, and H. Kazuyuki, "Nanomodification of glass using fs laser," Int. J. Appl. Glass Sci. **4**(3), 182–191 (2013).
24. B. Poumellec, M. Lancry, R. Desmarchelier, E. Hervé, and B. Bourguignon, "Parity violation in chiral structure creation under femtosecond laser irradiation in silica glass?" Light: Sci. Appl. **5**(11), e16178 (2016).
25. M. Beresna, M. Gecevičius, P. G. Kazansky, and T. Gertus, "Radially polarized optical vortex converter created by femtosecond laser nanostructuring of glass," Appl. Phys. Lett. **98**(20), 201101 (2011).
26. M. Beresna, M. Gecevičius, and P. G. Kazansky, "Polarization sensitive elements fabricated by femtosecond laser nanostructuring of glass," Opt. Mater. Express **1**(4), 783–795 (2011).
27. M. Lancry, R. Desmarchelier, K. Cook, B. Poumellec, and J. Canning, "Compact birefringent waveplates photo-induced in silica by femtosecond laser," Micromachines **5**(4), 825–838 (2014).
28. F. Zhang, Y. Yu, C. Cheng, Y. Dai, and J. Qiu, "Fabrication of polarization-dependent light attenuator in fused silica using a low-repetition-rate femtosecond laser," Opt. Lett. **38**(13), 2212–2214 (2013).
29. Y. Shimotsuma, M. Sakakura, P. G. Kazansky, M. Beresna, J. Qiu, K. Miura, and K. Hirao, "Ultrafast manipulation of self-assembled form birefringence in glass," Adv. Mater. **22**(36), 4039–4043 (2010).
30. G. Cerullo, R. Osellame, S. Taccheo, M. Marangoni, D. Polli, R. Ramponi, P. Laporta, and S. De Silvestri, "Femtosecond micromachining of symmetric waveguides at 1.5 μm by astigmatic beam focusing," Opt. Lett. **27**(21), 1938–1940 (2002).
31. R. Osellame, S. Taccheo, M. Marangoni, R. Ramponi, P. Laporta, D. Polli, S. De Silvestri, and G. Cerullo, "Femtosecond writing of active optical waveguides with astigmatically shaped beams," J. Opt. Soc. Am. B **20**(7), 1559–1567 (2003).
32. A. R. De la Cruz, A. Ferrer, J. Del Hoyo, J. Siegel, and J. Solis, "Modeling of astigmatic-elliptical beam shaping during fs-laser waveguide writing including beam truncation and diffraction effects," Appl. Phys. A **104**(2), 687–693 (2011).
33. R. Keil, Y. Lahini, Y. Shechtman, M. Heinrich, R. Pugatch, F. Dreisow, A. Tünnermann, S. Nolte, and A. Szameit, "Perfect imaging through a disordered waveguide lattice," Opt. Lett. **37**(5), 809–811 (2012).
34. J. Guan, X. Liu, P. S. Salter, and M. J. Booth, "Hybrid laser written waveguides in fused silica for low loss and polarization independence," Opt. Express **25**(5), 4845–4859 (2017).
35. R. Heilmann, C. Greganti, M. Gräfe, S. Nolte, P. Walther, and A. Szameit, "Tapering of femtosecond laser-written waveguides," Appl. Opt. **57**(3), 377–381 (2018).
36. I. Mansour and F. Caccavale, "An improved procedure to calculate the refractive index profile from the measured near-field intensity," J. Lightwave Technol. **14**(3), 423–428 (1996).
37. E. Knill, R. Laflamme, and G. J. Milburn, "A scheme for efficient quantum computation with linear optics," Nature **409**(6816), 46–52 (2001).
38. J. L. Dodd, T. C. Ralph, and G. Milburn, "Experimental requirements for grover's algorithm in optical quantum computation," Phys. Rev. A **68**(4), 042328 (2003).
39. J. L. O'brien, "Optical quantum computing," Science **318**(5856), 1567–1570 (2007).
40. J. H. Burnett, Z. H. Levine, and E. L. Shirley, "Intrinsic birefringence in calcium fluoride and barium fluoride," Phys. Rev. B **64**(24), 241102 (2001).
41. J. Qiu, P. Kazanski, J. Si, K. Miura, T. Mitsuyu, K. Hirao, and A. L. Gaeta, "Memorized polarization-dependent light scattering in rare-earth-ion-doped glass," Appl. Phys. Lett. **77**(13), 1940–1942 (2000).
42. M. Beresna, M. Gecevičius, M. Lancry, B. Poumellec, and P. Kazansky, "Broadband anisotropy of femtosecond laser induced nanogratings in fused silica," Appl. Phys. Lett. **103**(13), 131903 (2013).
43. A. Champion, M. Beresna, P. Kazansky, and Y. Bellouard, "Stress distribution around femtosecond laser affected zones: effect of nanogratings orientation," Opt. Express **21**(21), 24942–24951 (2013).
44. B. McMillen and Y. Bellouard, "On the anisotropy of stress-distribution induced in glasses and crystals by non-ablative femtosecond laser exposure," Opt. Express **23**(1), 86–100 (2015).
45. A. Arbabi, Y. Horie, M. Bagheri, and A. Faraon, "Dielectric metasurfaces for complete control of phase and polarization with subwavelength spatial resolution and high transmission," Nat. Nanotechnol. **10**(11), 937–943 (2015).
46. L. Sansoni, F. Sciarrino, G. Vallone, P. Mataloni, A. Crespi, R. Ramponi, and R. Osellame, "Polarization entangled state measurement on a chip," Phys. Rev. Lett. **105**(20), 200503 (2010).
47. P. O. Boykin, T. Mor, M. Pulver, V. Roychowdhury, and F. Vatan, "On universal and fault-tolerant quantum computing: a novel basis and a new constructive proof of universality for shor's basis," in *Foundations of Computer Science, 1999. 40th Annual Symposium on* (IEEE, 1999), pp. 486–494.
48. R. Drevinskas and P. G. Kazansky, "High-performance geometric phase elements in silica glass," APL Photonics **2**(6), 066104 (2017).

Optical Materials EXPRESS

49. C.-K. Hong, Z.-Y. Ou, and L. Mandel, "Measurement of subpicosecond time intervals between two photons by interference," Phys. Rev. Lett. **59**(18), 2044–2046 (1987).
50. S. Barz, "Quantum computing with photons: introduction to the circuit model, the one-way quantum computer, and the fundamental principles of photonic experiments," J. Phys. B: At., Mol. Opt. Phys. **48**(8), 083001 (2015).